Assessment of aortic valve pressure overload and leaflet functions in an ix vivo beating heart loaded with a continuous flow cardiac assist device

European Journal of Cardio-Thoracic Surgery 45 (2014) 377–383
doi:10.1093/ejcts/ezt355 Advance Access publication 30 June 2013

ORIGINAL ARTICLE

Assessment of aortic valve pressure overload and leaflet functions in an *ex vivo* beating heart loaded with a continuous flow cardiac assist device

Egemen Tuzun[a,b,c,*], Kim Pennings[b,c], Sjoerd van Tuijl[b], Jurgen de Hart[d], Marco Stijnen[b], Frans van de Vosse[b], Bas de Mol[b,c] and Marcel Rutten[b]

[a] Texas Institute for Preclinical Studies, Texas A&M University, College Station, TX, USA
[b] Department of Biomedical Engineering, Eindhoven University of Technology, Netherlands
[c] Department of Cardiothoracic Surgery, Academic Medical Center, Amsterdam, Netherlands
[d] HemoLab Cardiovascular Engineering, Eindhoven, Netherlands

* Corresponding author. 800 Raymond Stotzer Suite 2075, College Station, TX 77843, USA. Tel: +1-979-458 5754; fax: +1-979-845 6522; e-mail: egemen.tuzun@tamu.edu (E. Tuzun).

Received 25 March 2013; received in revised form 16 May 2013; accepted 28 May 2013

Abstract

OBJECTIVES: Aortic valve regurgitation, fusion and thrombosis are commonly reported clinical complications after continuous flow ventricular assist device implantations; however, the complex interaction between reduced pulsatile flow physiology and aortic valve functions has not been studied experimentally. To address this, a continuous flow left ventricular assist device was implanted in four swine *ex vivo* beating hearts and then operated at baseline (device off, no flow) and at device speeds ranging between 8500 and 11 500 rpm under healthy and experimentally created failing heart conditions.

METHODS: At baseline and after each speed increase, aortic, left ventricular, left atrial and pulse pressure signals were monitored to assess the haemodynamic status of the *ex vivo* heart, aortic valve opening time and the transvalvular pressure changes. Aortic root and device flows were recorded with flow probes. Left ventricular pressure–volume loops were measured with a conductance catheter. Changes in aortic leaflet motion and end-diastolic aortic root diameter were recorded with epicardial echocardiography.

RESULTS: A two-chamber healthy and failing *ex vivo* beating heart model was successfully created. At increasing device flows, aortic valve open time steadily decreased from 36 ± 7% of the baseline cardiac cycle to 0% at 11 500 rpm in the healthy heart and from 18 ± 16 to 0% in failing heart mode ($P < 0.05$). Aortic transvalvular pressure increased from 25 ± 5 mmHg (baseline) to 67 ± 7 mmHg (11 500 rpm) in the healthy heart and from 10 ± 9 mmHg (baseline) to 73 ± 8 mmHg (11 500 rpm) in failing heart mode ($P < 0.05$). Aortic root diameters were significantly increased at speeds exceeding 10 500 rpm in the healthy heart mode ($P < 0.05$ vs baseline) and approached statistical significance in failing hearts.

CONCLUSIONS: Increasing assist device flows resulted in pressure overload above the aortic leaflets, impaired leaflet functions, caused aortic root dilatation and altered leaflet coaptation at the central portion of the aortic valve in both modes. We conclude that the deleterious effect of the reduced pulsatile flow on the aortic valve functions and haemodynamics is immediate and such an insult may explain the structural changes of the aortic valve causing leaflet fusion and/or regurgitation in the chronic phase.

Keywords: Aortic valve • Leaflet functions • *Ex vivo* beating heart • Continuous flow • Cardiac assist device

INTRODUCTION

Mechanical circulatory support with ventricular assist devices (VADs), either pulsatile or continuous flow, is an accepted therapeutic option for the patients who are not candidates for heart transplantation due to the immediate need for cardiac support and/or donor shortage [1, 2]. After the introduction of continuous-flow VADs into the clinic, major complications such as infection and/or thromboembolic events significantly decreased in patients implanted with those devices [3]. However, the aortic valve regurgitation, fusion or stenosis are still common complications reported with an incidence of 11% at 6 months and 51% at 18 months after continuous flow VAD implantations [4, 5]. Yet, little is known about the association of those complications with continuous or reduced flow physiology, nevertheless it is likely that the altered haemodynamics are leading to dysfunctional remodelling of the aortic valve, as reported by several investigators [6–8]. Unfortunately, previous *in vitro* or postmortem studies performed with artificial valves and ventricles are not precise enough to simulate the real clinical scenario and dynamic tissue properties under continuous flow VAD support. On the other hand, the clinical reports lack a description of the mechanisms of the aortic

valve-continuous flow VAD interaction due to the unquestionable ethical restrictions on unnecessary invasive interventions in humans for research purposes. In order to overcome the above-mentioned problems and better simulate the real clinical scenario, we used a porcine *ex vivo* beating heart model (PhysioHeart, HemoLab) [9] loaded with a continuous flow VAD and assessed the haemodynamics during the aortic valve-continuous flow VAD interaction in healthy and failing heart conditions.

MATERIALS AND METHODS

Animals

Four domestic Dutch landrace hybrid adult pig hearts were obtained from pigs that were slaughtered for human consumption. The protocols at the slaughterhouse and laboratory follow EC regulations 1774/2002 regarding the use of slaughterhouse animal material for diagnosis and research, supervised by the Dutch Government (Dutch Ministry of Agriculture, Nature and Food Quality) and are approved by the associated legal authorities of animal welfare (Food and Consumer Product Safety Authority). These protocols prevent additional animal suffering and sacrifice in performing the experiments. The slaughterhouse procedures were carried out under the supervision of the representatives (veterinary officers) of the regulatory authorities.

Preparation of isolated hearts

A detailed description of the preparation has been published previously [9]. Briefly, following stunning the pigs (weighing 100 ± 10 kg) with an electroshock and hanging them on one hind leg and incising the carotid artery for exsanguination till death, the thorax was opened by a parasternal incision. The hearts (weighing 420 ± 30 g) were then removed en bloc, usually still beating and preparation was started at the slaughterhouse. After opening the pericardial sack the heart was immediately cooled topologically in ice slush. The pulmonary artery was cut just before the bifurcation while the aorta was cut at the level of the first supra-aortic vessels and subsequently cannulated for administration of 1 l of cold cardioplegic solution (4°C Modified StThomas2 added with 5000 IU of Heparin) to the coronary arteries at a pressure of 80 mmHg. This procedure was optimized such that warm ischaemic time never exceeded 5 min and was generally kept below 3 min. Meanwhile, 5 l of fresh blood for reperfusion was collected from subsequently slaughtered pigs, since pigs lack the antibodies against different blood group factors. The heart and blood (heparinized with 5000 IU/l) were then stored cold during transportation to the laboratory.

Each heart was placed in an insulated container filled with ice-cold saline solution to reduce damage to the heart tissue due to ischaemia. The aorta and the left atrium were cannulated using ¾-in cannulas to connect the left side of the heart to an *ex vivo* circuit. The pulmonary artery was cannulated to measure coronary sinus outflow. Epicardial pacing wires (Ethicon, Inc., Somerville, NJ, USA) were placed on the aorta, left atrium and left ventricle (LV) to monitor electrical activity and to pace the heart (if necessary).

A Micromed DeBakey continuous flow VAD that was described in detail elsewhere [10] was used for all experiments. The inflow cannula was inserted into the LV via the ventricular apex, and the sewing ring was attached to the ventricle using 2/0 TiCron teflon-pledgeted sutures. Once the implantation procedure was completed, the outflow graft was mounted 15 cm distal to the aortic valve with a 90° angle.

Connection of isolated hearts to the circuit

The perfusion circuit (Fig. 1) was assembled and primed with a normothermic (38°C) 1 : 1 mixture of Krebs–Henseleit buffer (4.0 ± 0.5 l) (Sigma-Aldrich, Inc., St. Louis, MO, USA) and heparinized autologous blood (4.0 ± 0.5 l) (final hematocrit, 15 ± 1%; pH, 7.40 ± 0.05) supplemented with insulin (0.32 units/l). At room temperature, each pig heart was suspended in an elastic sleeve, and the left side of the heart was connected to the circuit as follows. The aortic cannula was connected to the circuit to induce the modified Langendorff mode. The heart was perfused retrogradely from the aorta in order to keep the coronary perfusion pressure at 70 mmHg. Following 5 min of modified Langendorff mode perfusion, regular myocardial contractile activity was reestablished, and the left atrial cannula was connected to the circuit to induce the beating-ejecting mode. If needed, the heart was defibrillated with 10J. The heart was then perfused anterogradely from the LV into the coronary arteries through the aorta. The heights of the preload and afterload reservoirs were adjusted to create a preload of 10–20 mmHg and an afterload of 100–120 mmHg.

Perfusion of isolated hearts on the *ex vivo* circuit

In this two-chamber beating-ejecting mode, the LV ejected the perfusate into the aortic cannula, where aortic pressure (AoP) was measured. The compliance chamber, placed in series between the aorta and the afterload reservoir, partially corrected the cyclic fluctuations in pump pressure. Through an overflow tube in the afterload reservoir, the perfusate was collected into a reservoir and pumped by the first roller pump (Sarns 9000 Perfusion System, 3M) into the venous reservoir, where it then passed through an arterial filter (AFFINITY® Arterial 38-µm blood filter, Medtronic). A centrifugal pump routed the perfusate into the oxygenator (AFFINITY® NT Oxygenator, Medtronic), which contained

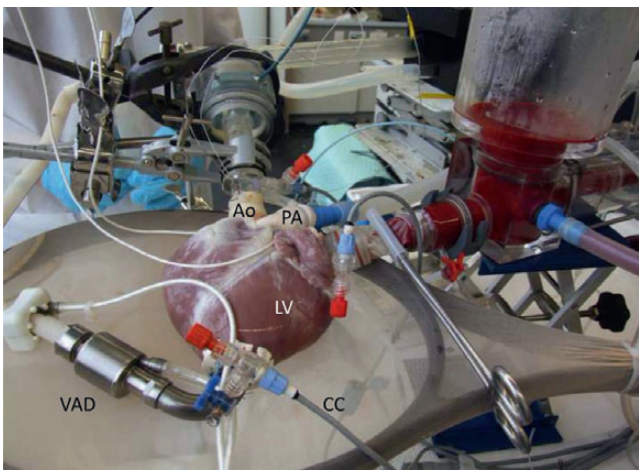

Figure 1: *Ex vivo* beating heart perfusion circuit loaded with a left ventricular assist device. VAD: ventricular assist device; CC: conductance catheter; Ao: aorta; PA: pulmonary artery; LV: left ventricle.

95% oxygen and 5% carbon dioxide. The blood glucose level was maintained manually between 5 and 7 mmol/l by the addition of glucose–insulin–potassium (GIK). The oxygenator was connected to the heater–cooler, which kept the perfusate at 37°C by recirculating heated water through the oxygenator. The heated and oxygenated perfusate was then pumped by the second roller pump back into the preload reservoir, where its temperature was measured. From the preload reservoir, the left atrium was supplied with oxygenated perfusate. Coronary venous perfusate was returned to the circuit through the cannula leading from the pulmonary artery to the reservoir. The mean coronary flow was measured with an ultrasound flow probe, and the pressure was measured ~15 cm upstream from the coronary ostia with a pressure sensor (P10EZ-1, Becton Dickinson Medical). The third roller pump was used to fill the afterload reservoir initially for modified Langendorff-mode perfusion. The preload reservoir could be emptied into the reservoir through an overflow tube. Left atrial pressure (LAP) was measured with a pressure transducer connected to the left atrial cannula.

Data collection

The following data are collected at the baseline (VAD is not running and outflow graft is clamped) and with the VAD running at speeds (outflow graft clamp is unclamped) from 8500, 9500, 10 500 and 11 500 rpm during measurements on healthy heart and failing heart, with 2 min of interval between each speed change. Once haemodynamic steady state was reached in beating-ejecting mode, AoP, LAP, left ventricular pressure (LVP), pulse pressure (PP) electrocardiography and heart rate (HR) were recorded continuously using a Labview-based data acquisition system (National Instruments, Austin, TX, USA). Electrophysiological signals were monitored as ECG-derived signals epicardial pacing leads. The aortic and LAPs were monitored with pressure sensors (P10EZ-1, Becton Dickinson Medical, Singapore). The LV pressure–volume (PV) loops were measured with a conductance catheter (CD Leycom, Netherlands), which was introduced into the ventricle transapically by means of a needle. The aortic flow (Q_a) was measured ~100 mm distal of the aortic valve annulus by an ultrasonic flow sensor (MA28PAX, Transonic Systems, Inc.) VAD flow (Q_{VAD}) is measured from the outflow graft with the Micromed flow probe. Total cardiac output (CO) was calculated (in l/min) as follows:

$$CO = Q_c + Q_a + Q_{vad}$$

where Q_c is coronary blood flow.

Aortic leaflet motions and end-diastolic aortic root diameter (mm) were recorded with epicardial echocardiography with a curved array probe (Picus Ultrasound Scanner, ESAOTE, Europe). Aortic valve open time was calculated with pressure signals. Transvalvular pressure (TP) was calculated with AoP and LVP measurements.

Induction of *ex vivo* heart failure

In three hearts, distal left anterior descending and circumflex obtuse margin coronary arteries were ligated and acute ischaemic heart failure was successfully created as detected by PV loops. One heart failed without any ischaemic induction, probably due to insufficient myocardial protection during the harvesting, transportation or preparation. Each experiment state is repeated once.

Statistics

The results are expressed in mean ± SD format. The reproducibility of the *ex vivo* measurements was determined using a paired *t*-test, comparing the two measurements done under the same conditions. A three-way ANOVA test is performed to calculate the significance of the haemodynamic parameters between healthy and failing conditions and different levels of LVAD support. Mean values of haemodynamic parameters were determined during measurements in four hearts at different pump speeds under either healthy or failing conditions. So for each measurement, it was defined in which heart the measurement was done, in what condition the particular heart was and what level of LVAD support was performed. A *P*-value <0.05 was considered statistically significant.

RESULTS

A two-chamber *ex vivo* beating heart mode was used for all hearts. Data were collected at two time intervals (first healthy, then failing heart condition) for each *ex vivo* experiment, while the hearts were kept in a beating heart mode for up to 4 h.

Baseline haemodynamic data in *ex vivo* healthy and failing heart conditions

During the baseline data collection, the shunt created between the aorta and LV apex (through the VAD) was closed by an arterial clamp to the outflow graft. The mean AoP, LVP and PP achieved at the baseline healthy heart conditions were 84 ± 8, 60 ± 7 and 38 ± 3 mmHg, respectively. These values were decreased to 64 ± 11, 54 ± 8 and 32 ± 5 mmHg, respectively, considering the failing heart ($P < 0.05$ for all parameters) (Fig. 2A and B). The mean baseline LAP values significantly increased after the creation of heart failure compared with healthy heart values (18 ± 7 vs 23 ± 10 mmHg, $P < 0.05$). Figs 3 and 4 show, respectively, the characteristic aortic and LVP waveforms and PV loops generated by the healthy and failing heart conditions in one experiment prior to VAD support. The mean total cardiac output obtained at the baseline under healthy heart conditions was 4.5 ± 0.9 l/min at a mean HR of 105 ± 3 bpm, with a corresponding mean stroke volume of 41.6 ± 8.3 ml. After the induction of heart failure, the mean cardiac output decreased to 3.8 ± 0.9 l/min, with a mean HR of 103 ± 1 bpm and a stroke volume of 36.9 ± 8.7 ml ($P < 0.05$ for both parameters). The changes at the CO, Q_a and Q_{VAD} before and after heart failure creation are summarized in Fig. 5. Correlation of these parameters with standard healthy and failing heart conditions indicated the functionality of the *ex vivo* beating heart platform and the validity of the acquired data.

Mean TP was 25 ± 5 and 10 ± 9 mmHg in healthy and failing heart conditions, respectively (Fig. 6).

Aortic valve open time was 36 ± 7% of the cardiac cycle in the healthy heart, which increased to 18 ± 16% in failing heart conditions as calculated by pressure signals (Fig. 7). Aortic leaflet function

and coaptation were normal in healthy and failing heart experiments. The baseline mean aortic root diameters were 28 mm and 23.7 ± 0.6 mm in healthy and failing hearts, respectively ($P < 0.05$) (Fig. 8).

Haemodynamic data after VAD support in *ex vivo* healthy and failing heart conditions

The mean AoP increased at increasing pump speeds with a corresponding decrease at the LVP and PP in healthy and failing hearts compared with baseline values as shown in Fig. 2A and B ($P < 0.05$ for all parameters). The mean LAP gradually and significantly decreased at increasing pump speeds in healthy and failing heart conditions ($P < 0.05$ vs baseline). Fig. 4 shows pressure–volume relations for the VAD-supported heart for one of the cases, where increasing pump speed decreased the ventricular pressure as well as the ventricular volume gradually in healthy and failing heart conditions. The mean Q_{VAD} significantly increased at increasing pump speeds in healthy and failing conditions ($P < 0.05$), along with a sharp decrease in Q_a flow ($P < 0.05$). The increase in the mean total cardiac output obtained at the increasing pump speeds was more pronounced in failing heart conditions compared with healthy hearts ($P < 0.05$). Depending on the extent of LV unloading, the Q_a flow gradually decreased and reversed direction at increasing VAD supports resulting in aortic regurgitation at speeds exceeding 9500 rpm in both healthy and failing conditions ($P < 0.05$ vs baseline) (Fig. 5A and B). The mean TP gradually and significantly increased from 25 ± 5 mmHg (baseline) to 67 ± 7 mmHg (11 500 rpm) in the healthy heart and from 10 ± 9 mmHg (baseline) to 73 ± 8 mmHg in failing heart conditions ($P < 0.05$ vs baseline) (Fig. 6). There was no statistically significant difference between healthy and failing groups in terms of TP ($P = 0.86$).

Aortic valve open time decreased from 36 ± 7% of the cardiac cycle to 0% in the healthy heart and from 18 ± 16% of the cardiac cycle to 0% in failing heart condition as calculated by pressure signals ($P < 0.05$ vs baseline) (Fig. 7). There was no statistically significant difference between healthy and failing groups in terms of aortic valve open time ($P = 0.45$).

Aortic valve open time root diameter increased from 28 ± 0.1 to 30.1 ± 0.9 mm at 10 500 rpm in the healthy heart mode ($P < 0.05$ vs baseline). At 11 500 rpm, the aortic root diameter decreased below the baseline level (28 ± 0.1 to 26.7 ± 0.9 mm, $P < 0.05$ vs baseline), along with an increase in retrograde Q_a flow and ventricular suction effect detected by echocardiography. Aortic root diameter increased from 23.7 ± 0.7 to 27.4 ± 1.9 mm at 10 500 rpm ($P < 0.05$ vs baseline) in the failing mode followed by a reduction as detected in healthy mode (23.7 ± 0.7 to 24.6 ± 0.7 mm, $P = 0.13$ vs baseline) (Fig. 8).

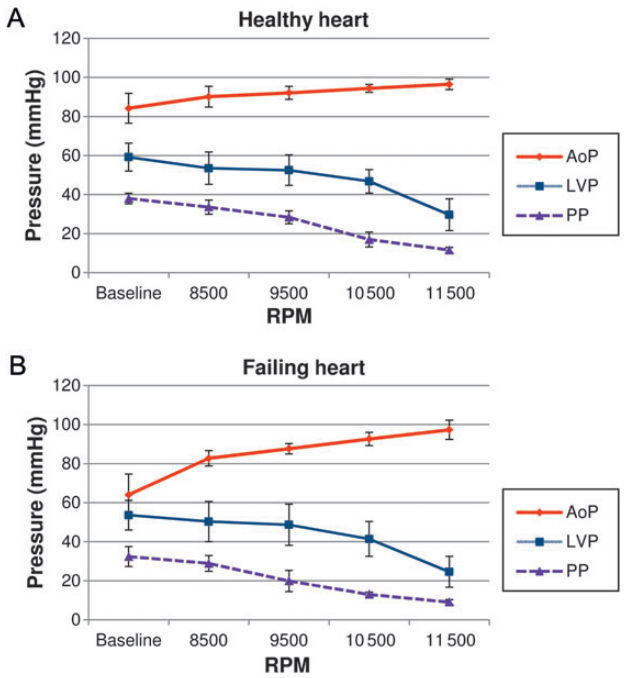

Figure 2: Mean aortic, left ventricular and pulse pressures at the baseline and increasing VAD supports in healthy (**A**) and failing (**B**) heart modes. ($P < 0.05$ vs baseline in all speeds.) AoP: mean aortic pressure; LVP: left ventricular pressure; PP: pulse pressure; VAD: ventricular assist device; RPM: rotation per minute.

DISCUSSION

In the *ex vivo* beating heart model (PhysioHeart, HemoLab) loaded with a continuous flow VAD, we were successfully able to simulate healthy and failing heart conditions. We demonstrated

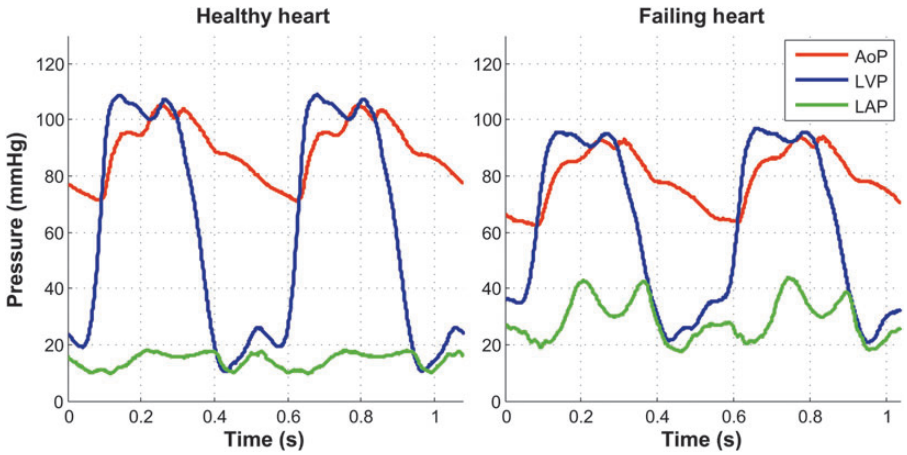

Figure 3: Typical left ventricular, aortic and left atrial pressure waveforms on healthy (left) and failing heart (right) modes. LVP: left ventricular pressure; AoP: aortic pressure; LAP: left atrial pressure.

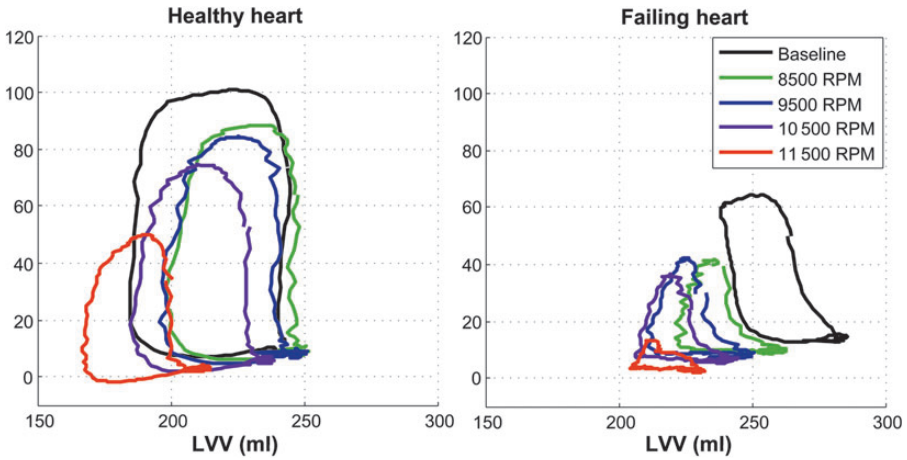

Figure 4: PV loops generated by the healthy (left) and failing (right) heart modes in one experiment before and after left VAD support. PV: pressure–volume; VAD: ventricular assist device; LVP: left ventricular pressure; LVV: left ventricular volume; RPM: rotation per minute.

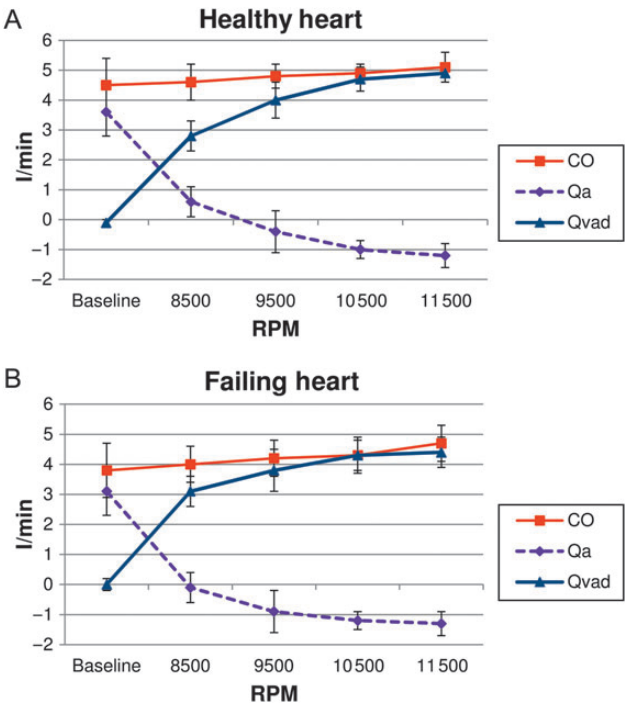

Figure 5: Total cardiac output, aortic and VAD flows at the baseline and increasing VAD supports in healthy (**A**) and failing (**B**) heart modes ($P < 0.05$ vs baseline in all speeds). CO: total cardiac output; Q_a: aortic flow; Q_{VAD}: ventricular assist device flow; VAD: ventricular assist device; RPM: rotation per minute.

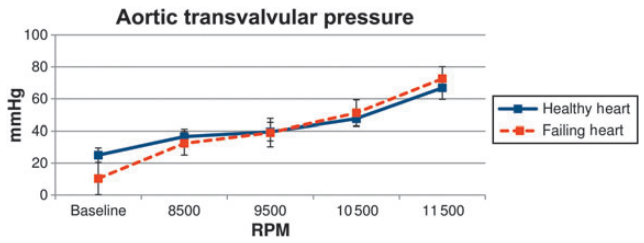

Figure 6: Aortic transvalvular pressures at the baseline and increasing VAD supports in healthy and failing heart modes ($P < 0.05$ vs baseline in all speeds). VAD: ventricular assist device; RPM: rotation per minute.

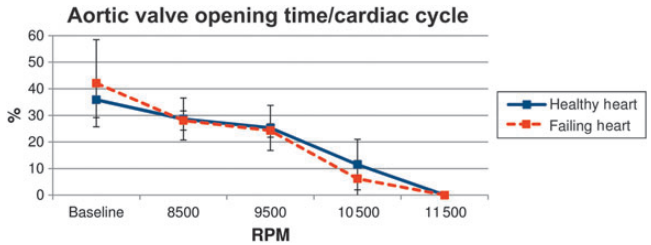

Figure 7: Aortic valve opening time per cardiac cycle at the baseline and increasing VAD supports in healthy and failing heart modes ($P < 0.05$ vs baseline in all speeds). VAD: ventricular assist device; RPM: rotation per minute.

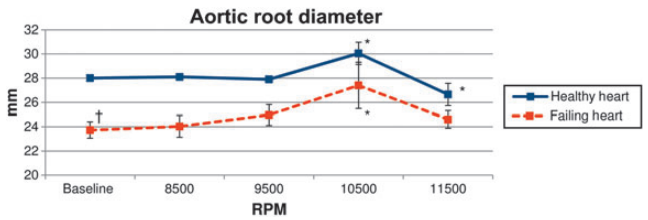

Figure 8: Aortic root diameter at the baseline and increasing VAD supports in healthy and failing heart modes ($^{\dagger}P < 0.05$ vs healthy; $^{*}P < 0.05$ vs baseline). VAD: ventricular assist device; RPM: rotation per minute.

that the pressure load on the aortic valve was almost 2.5 times higher than the baseline when the LV was fully unloaded, with a continuous flow VAD in healthy heart experiments, whereas the pressure load was seven times higher under failing heart conditions. With increasing VAD speeds, aortic valve open time reduced to zero, aortic root diameters were increased compared with baseline measurements and aortic leaflet motions were partially or completely impaired.

The aim of our study was to explore haemodynamic and functional changes in the duration and level of the diastolic pressure load on a normally functioning aortic valve being subjected to the non- or near-physiological hydrodynamic conditions imposed by a healthy and failing heart being assisted by a continuous flow VAD. Although we performed our preliminary studies on *in vitro* mock loop models [7], we believe that a mock-loop loaded with a mechanical valve and rigid tubes would not have sufficient haemodynamic similarity to a native heart valve to support our findings and to translate these into loads on a native valve.

Therefore, we chose this established model of an *ex vivo* beating heart model to better assess the aortic valve and continuous flow VAD interaction under more realistic conditions. In this study, we demonstrated that normal cardiac haemodynamic performance was achieved both qualitatively, in terms of pulse waveforms (Aop, LVAP, LAP), and quantitatively, in terms of average cardiac output and pressures (PV loops). In all but one heart, cardiac performance was controlled and kept at normal levels for up to 4 h, with only minor deterioration of haemodynamic performance. One heart developed early failure, possibly due to inadequate myocardial preservation. Furthermore, this model enabled us to use the epicardial echocardiography to assess the leaflet functions and flow-dependent morphological changes at the leaflets and aortic root such as flow stagnation, leaflet and aortic root dilatation and/or aortic regurgitation in response to VAD speed changes. Another advantage of the model is that we use fresh pig hearts acquired from a local slaughterhouse. Although different groups [11, 12] have reported that prolonged warm ischaemia may well be tolerated, none of their models were able to regain close to normal cardiac haemodynamics. We have experienced that it was essential to keep warm ischaemic time as short as possible because of clear haemodynamic deterioration of the heart performance. The use of slaughterhouse hearts was beneficial from a time, cost and ethical perspective [13], but also allowed us to have access to a virtually unlimited supply of fresh hearts.

Aortic valve commissural fusion and resultant insufficiency have recently begun to be considered complications of the prolonged use of the pulsatile or non-pulsatile left VADs, which may cause poor patient prognosis [14–16]. Previous *in vitro* and post-mortem studies suggested that increased pressure load above the aortic valve due to increased VAD flow may result in impaired aortic valve functions and opening, and consequently may lead to aortic valve fusion, thrombosis or incompetence [6–8]. Under normal physiological conditions, a constant tissue renewal in aortic valve leaflets is demonstrated while altered mechanical forces (i.e. hypertension) result in changes in their structural and biological properties [17–19]. Our haemodynamic data are closely correlated with previous *in vitro* studies that have demonstrated an increase in TVP along with a decrease in aortic valve open time and aortic blood flow at increasing VAD speeds and flows in healthy and failing heart conditions [7, 20]. Nevertheless, the aortic valve is a functional assembly composed of the three cusps, corresponding sinuses and the sinotubular junction. It is characterized not only by morphological features but also its functional properties, which together create an environment that is optimal for the distribution of diastolic pressure load, and assures proper and timely valve opening and closure [21]. Therefore, it is unlikely to assess precisely the complex interaction between constantly changing aortic valve geometry and continuous flow VADs in *in vitro* models. The uniqueness of our study is to show the real-time changes on the aortic leaflet shape and aortic root circumferential diameter along with the aortic leaflet functions under different VAD flow rates and hydrodynamic conditions with epicardial echocardiographic measurements. We have demonstrated that prior to the VAD support, failing hearts had significantly smaller aortic root diameters compared with the healthy hearts, which may be explained by the decreased aortic root pressure and wall tension secondary to the left ventricular failure. The initiation of VAD support resulted in pressure overload above the aortic valve, which caused flattening of the aortic leaflets, increase in aortic root diameter during diastole and retrograde flow through aortic leaflets due to altered leaflet coaptation in both healthy and failing hearts. The aortic root diameter decreased below baseline levels when the LV was overly unloaded at maximum VAD speeds due to a collapsed left ventricular outflow tract and increased retrograde aortic flow. Under physiological conditions, the radial length of the aortic leaflets does not change significantly during systolic aortic flow; however, when the leaflets close and coapt under increasing pressure, the radial length increases during diastole [18], but as shown in our study, altered haemodynamic changes above and below the aortic valve may result in aortic root dilatation, leaflet deformation and aortic regurgitation immediately after continuous flow VAD implantation. Considering that aortic valve fusion and/or regurgitation is reported to be a time-dependent process with increasing severity over time that may be related to continued valve remodelling from altered haemodynamics causing prolonged leaflet coaptation, phenotypic remodelling of valvular endothelial cells promoting local fibrosis or inflammatory processes [22–24], our data may be valuable to show that the onset of this process is immediate with increasing pump flows/speeds. Therefore, during clinical patient follow-up, we may suggest that performing regular echocardiographic assessments and keeping the pump speed at the lowest level in order to provide an optimum cardiac output without compromising the aortic leaflet functions will be a rational preventive measure to avoid valve fusion and/or regurgitation after VAD implantations.

The present study has some limitations. First, the VADs are designed to be used in patients with end-stage cardiac failure; therefore, our present results, obtained in a healthy/failing *ex vivo* heart model, may not be directly applicable to the clinical setting. Second, we examined the immediate effects of the continuous-flow LVAD implantation; therefore, we cannot draw any conclusions about the long-term effects of continuous flow LVADs on aortic valve functions and structures. This limitation might be addressed in the future by establishing chronic heart failure animal models in which the chronic effects of the continuous flow VADs on aortic valve function and structure could be assessed. Third, our conclusions were based on a relatively small number of *ex vivo* hearts; nevertheless, because this is the first and only *ex vivo* study focused on this topic, we believe that the very consistent trends in even four *ex vivo* hearts with healthy and failing settings are important. Fourth, it must be taken into consideration that in *ex vivo* heart studies, the aortic root is completely dissected free from its surrounding structures such as pericardium and pulmonary artery, which may indirectly affect the normal aortic root configuration during the cardiac cycle and may interfere with the haemodynamic and echocardiographic measurements. And finally, it must be considered that the outflow graft anastomosis angle, location, diameter and the distance to the aortic valve may affect the haemodynamic and flow measurements. Although our 90° anastomotic angle is not a perfect simulation of the clinical implant scenario, we think that the distance between the outflow graft anastomosis and the aortic valve is relatively long (15 cm) in our *ex vivo* study compared with clinical cases; therefore, anastomotic variables may not have a significant influence on haemodynamic measurements.

CONCLUSION

Increasing levels of continuous flow VAD support result in an immediately increased pressure overload on the aortic valve and reduced aortic valve opening time during the cardiac cycle along with an end-diastolic aortic root dilatation, leaflet flattening and

central aortic regurgitation. It is likely that chronically altered aortic valve mechanics and functions may explain structural valve changes causing leaflet fusion, thrombosis and/or regurgitation reported in the clinical situation.

Conflict of interest: none declared.

REFERENCES

[1] Frazier OH, Rose EA, Oz MC, Dembitsky W, McCarthy P, Radovancevic B, Poirier VL, Dasse KA; HeartMate LVAS Investigators. Multicenter clinical evaluation of the HeartMate vented electric left ventricular assist system in patients awaiting heart transplantation. J Thorac Cardiovasc Surg 2001; 122:1186–95.

[2] Frazier OH, Myers TJ, Westaby S, Gregoric ID. Use of the Jarvik 2000 left ventricular assist system as a bridge to heart transplantation or as destination therapy for patients with chronic heart failure. Ann Surg 2003;237: 631–7.

[3] John R, Kamdar F, Liao K, Colvin-Adams M, Boyle A, Joyce L. Improved survival and decreasing incidence of adverse events with the HeartMate II left ventricular assist device as bridge-to-transplant therapy. Ann Thorac Surg 2008;86:1227–34.

[4] Mudd JO, Cuda JD, Halushka M, Soderlund KA, Conte JV, Russell SD. Fusion of aortic valve commissures in patients supported by a continuous axial flow left ventricular assist device. J Heart Lung Transplant 2008;27: 1269–74.

[5] Cowger J, Pagani FD, Haft JW, Romano MA, Aaronson KD, Kolias TJ. The development of aortic insufficiency in LVAD-supported patients. Circ Heart Fail 2010;3:668–74.

[6] John R, Mantz K, Eckman P, Rose A, May-Newman K. Aortic valve pathophysiology during left ventricular assist device support. J Heart Lung Transplant 2010;29:1321–9.

[7] Tuzun E, Rutten M, Dat M, van de Vosse F, Kadipasaoglu C, de Mol B. Continuous-flow cardiac assistance: effects on aortic valve function in a mock loop. J Surg Res 2011;171:443–7.

[8] May-Newman K, Enriquez-Almaguer L, Posuwattanakul P, Dembitsky W. Biomechanics of the aortic valve in the continuous flow VAD-assisted heart. ASAIO J 2010;56:301–8.

[9] de Hart J, de Weger A, van Tuijl S, Stijnen JM, van den Broek CN, Rutten MCde Mol BA. An *ex vivo* platform to simulate cardiac physiology: a new dimension for therapy development and assessment. Int J Artif Organs 2011;34:495–505.

[10] Noon GP, Morley DL, Irwin S, Abdelsayed SV, Benkowski RJ, Lynch BE. Clinical experience with the MicroMed DeBakey ventricular assist device. Ann Thorac Surg 2001;71(Suppl. 3):S133–8.

[11] Rosenstrauch D, Akay HM, Bolukoglu H, Behrens L, Bryant L, Herrera P, Eya K, Tuzun E, Clubb FJ Jr, Radovancevic B, Hrazier OH, Kadipasaoglu K. *Ex vivo* resuscitation of adult pig hearts. Tex Heart Inst J 2003;30:121–7.

[12] Henze E, Schoser K, Lietzenmayer R, Schnur G, Sauer M, Kunz R, Clauser MAdam WE. Studies of myocardial metabolism using P-31-NMR spectroscopy and a simple heart perfusion model of slaughtered animals—an approach to avoiding in vivo animal experiments. Z Kardiol 1989;78: 553–60.

[13] Modersohn D, Eddicks S, Grosse-Siestrup C, Ast I, Holinski S, Konertz W. Isolated hemoperfused heart model of slaughterhouse pigs. Int J Artif Organs 2001;24:215–21.

[14] Letsou GV, Connelly JH, Delgado RM III, Myers TJ, Gregoric ID, Smart FW, Frazier OH. Is native aortic valve commissural fusion in patients with long-term left ventricular assist devices associated with clinically important aortic insufficiency? J Heart Lung Transplant 2006;25:395.

[15] Baradarian S, Dembitsky WP, Jaski B, Abolhoda A, Adamson R, Chillcot S, Daily PO. Left ventricular outflow tract obstruction associated with chronic ventricular assist device support. ASAIO J 2002;48:665–7.

[16] Toda K, Fujita T, Domae K, Shimahara Y, Kobayashi J, Nakatani T. Late aortic insufficiency related to poor prognosis during left ventricular assist device support. Ann Thorac Surg 2011;92:929–34.

[17] Schneider PJ, Deck JD. Tissue and cell renewal in the natural aortic valve of rats: an autoradiographic study. Cardiovasc Res 1981;15:181–9.

[18] Thubrikar MJ, Aouad J, Nolan SP. Comparison of the in vivo and in vitro mechanical properties of aortic valve leaflets. J Thorac Cardiovasc Surg 1986;92:29–36.

[19] Weston MW, Yoganathan AP. Biosynthetic activity in heart valve leaflets in response to in vitro flow environments. Ann Biomed Eng 2001;29: 752–63.

[20] Zamarripa-Garcia MA, Enriquez LA, Dembitsky W, May-Newman K. The effect of aortic valve incompetence on the hemodynamics of a continuous flow ventricular assist device in a mock circulation. ASAIO J 2008;54: 237–44.

[21] Robicsek F, Thubrikar MJ. Etiology of degenerative disease of the tri-leaflet aortic valve: a simple explanation for a complex problem. Z Kardiol 2001; 90(Suppl. 6):35–8.

[22] Connelly JH, Abrams J, Klima T, Vaughn WK, Frazier OH. Acquired commissural fusion of aortic valves in patients with left ventricular assist devices. J Heart Lung Transplant 2003;22:1291–5.

[23] Butcher JT, Penrod AM, Garcia AJ, Nerem RM. Unique morphology and focal adhesion development of valvular endothelial cells in static and fluid flow environments. Arterioscler Thromb Vasc Biol 2004;24:1429–34.

[24] Butcher JT, Nerem RM. Valvular endothelial cells and the mechanoregulation of valvular pathology. Phil Trans R Soc Lond B Biol Sci 2007;362: 1445–57.